



**HAL**  
open science

## Battery sizing for a stand alone passive wind system using statistical techniques

Malek Belouda, Jamel Belhadj, Bruno Sareni, Xavier Roboam

► **To cite this version:**

Malek Belouda, Jamel Belhadj, Bruno Sareni, Xavier Roboam. Battery sizing for a stand alone passive wind system using statistical techniques. 8th International Conference on System, Signal and Devices - SSD'11, Mar 2011, Sousse, Tunisia. pp.1-7, 10.1109/SSD.2011.5767373 . hal-04041484

**HAL Id: hal-04041484**

**<https://hal.science/hal-04041484>**

Submitted on 22 Mar 2023

**HAL** is a multi-disciplinary open access archive for the deposit and dissemination of scientific research documents, whether they are published or not. The documents may come from teaching and research institutions in France or abroad, or from public or private research centers.

L'archive ouverte pluridisciplinaire **HAL**, est destinée au dépôt et à la diffusion de documents scientifiques de niveau recherche, publiés ou non, émanant des établissements d'enseignement et de recherche français ou étrangers, des laboratoires publics ou privés.



**Open Archive TOULOUSE Archive Ouverte (OATAO)**  
OATAO is an open access repository that collects the work of Toulouse researchers and makes it freely available over the web where possible.

This is an author-deposited version published in : <http://oatao.univ-toulouse.fr/>  
Eprints ID : 9251

To link to this article : DOI:10.1109/SSD.2011.5767373  
URL : <http://dx.doi.org/10.1109/SSD.2011.5767373>

To cite this version :  
Belouda, Malek and Belhadj, Jamel and Sareni, Bruno and Roboam, Xavier *Battery sizing for a stand alone passive wind system using statistical techniques*. (2011) In: 8th International Conference on System, Signal and Devices - SSD'11, 22-24 march 2011, Sousse, Tunisia.

Any correspondence concerning this service should be sent to the repository administrator: [staff-oatao@listes.diff.inp-toulouse.fr](mailto:staff-oatao@listes.diff.inp-toulouse.fr)

# Battery sizing for a stand alone passive wind system using statistical techniques

*Malek Belouda<sup>(1)</sup>, Jamel Belhadj<sup>(1),(2)</sup>, Bruno Sareni<sup>(3)</sup>, Xavier Roboam<sup>(3)</sup>*

(1) Laboratoire des systèmes électriques (LSE) ENIT BP 37, Le Belvédère 1002 Tunis, Tunisia.

University of Tunis « ElManar » ; [malek.belouda@gmail.com](mailto:malek.belouda@gmail.com), [Jamel.Belhadj@esstt.rnu.tn](mailto:Jamel.Belhadj@esstt.rnu.tn)

(2) ESSTT, DGE, BP 56, Montfleury 1008, Tunis, Tunisia. University of Tunis

(3) Université de Toulouse , LAPLACE UMR CNRS – INP – UPS site ENSEEIHT – 2, Rue Charles Camichel 31071 TOULOUSE – France [roboam@laplace.univ-tlse.fr](mailto:roboam@laplace.univ-tlse.fr), [sareni@laplace.univ-tlse.fr](mailto:sareni@laplace.univ-tlse.fr)

## ABSTRACT

In this paper, an original optimization method to jointly determine a reduced study term and an optimum battery sizing is investigated. This storage device is used to connect a passive wind turbine system with a stand alone network. A Weibull probability density function is used to generate different wind speed data. The passive wind system is composed of a wind turbine, a permanent magnet synchronous generator feeding a diode rectifier associated with a very low voltage DC battery bus. This study is essentially based on a similitude model applied on an 8 kW wind turbine system. Our reference model is taken from a 1.7 kW optimized system. The wind system generated power and the load demand are coupled through a battery sized using a statistical approach.

**Index Terms** — Wind energy systems, energy storage, mixed-reduced model, similitude approach, statistical methods.

## 1. INTRODUCTION

Small renewable energy systems as wind turbine, photovoltaic or hybrid sources are actually very useful especially for remote areas for electricity production pumping and water desalination.

Usually, these systems are not sized from designer's expertise, and do not take into account wind/irradiance potentials and load demand. There is an extensive range of configurations that allows tracking the maximum power operation through corresponding MPPT strategies. Nevertheless, active structures present a consequent system cost due to the use of active power and control devices [1-4].

In this paper, we consider an 8 kW full passive wind turbine battery charger without active control and with minimum number of sensors. The system parameters are obtained by similitude from a 1.7 kW optimized passive structure [5]. A battery sizing procedure based on a statistical approach is used for associating the wind energy potential with a given load power demand.

The remaining of the paper is organized as follows. The passive wind system, wind speed generation and load demand are described in section 2. In the third

section, models simulating the wind turbine systems are presented. Especially, the similitude model of the mixed reduced model is explained. Section 4 is dedicated to the algorithm and the statistical methodology used for the battery sizing. The results obtained from this approach are summarized and shown in section 5.

## 2. PASSIVE WIND SYSTEM STRUCTURE

### 2.1. Wind turbine structure

In order to minimize the system cost and to maximize reliability, a passive wind turbine with very low DC output voltage (less than 50 V) is considered. .

To offer an autonomous system operation for remote applications, a battery bank is coupled to the DC bus at the output of the diode bridge rectifier. This structure is characterized by a minimum of sensors and is operating without controlled power devices. An integrated optimal design approach using multiobjective genetic algorithm was used to size a 1.7 kW system allowing to maximize energy efficiency and to minimize the system mass [5]. This system will be taken as reference device in our similitude model.

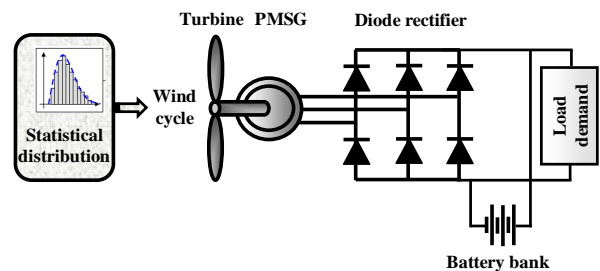


Figure 1. Passive wind turbine system structure.

### 2.2. Wind speed profile generation

In this study the wind speed is described with statistical methods [6, 7, 16] from the wind energy potential features. The synoptic of the random process generation of the Wind speed is illustrated in Figure 2. The wind speed sequence is obtained by inverse transformation of the wind speed probability density function. This discrete sequence is sampled with a period  $T = 30\text{min}$ . Note that this sampling period has to be higher than time constants associated with turbulence phenomena. Finally, continuous wind speed data are

obtained from the previous discrete sequence using a cubic interpolation with a period  $T_i = 18$  s.

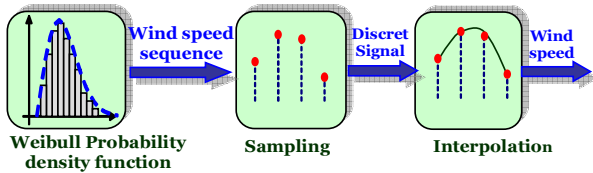


Figure 2. Wind speed generation methodology.

Wind speed data can be predicted by several statistical distributions models from the wind energy potential at a particular location. The most commonly used distribution is the Weibull law that can be expressed by the following probability density function (Wpd) [9]:

$$Wpd(v) = \frac{k}{c} \left(\frac{v}{c}\right)^{k-1} \cdot e^{-\left(\frac{v}{c}\right)^k} \quad (1)$$

where  $c$  is a scale factor (m/s),  $k$  represents a shape factor and  $v$  denotes the wind speed (m/s). In this study the Weibull parameters  $c$  and  $k$  are respectively set to 9 and 2. Figure 3 shows the corresponding probability density function with those parameters.

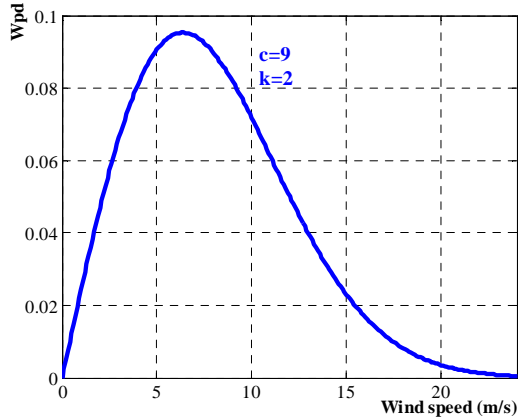


Figure 3. Typical Weibull probability density function relative to the wind energy potential of a given location.

The discrete generator of random numbers  $W(c,k)$  fulfilling the Weibull law is obtained by inverse transformation as follows:

$$W(c,k) = c(-\text{Log}(U(0,1)))^{1/k} \quad (2)$$

where,  $U(0,1)$  represents a random number lying in the interval  $]0,1[$  with uniform probability.

The complete procedure for generating a wind speed profile of one day duration is illustrated in Figure 4. It should be noted that this representation only considers the “main energetic behaviour” of wind. It does not take into account disturbance phenomena resulting from turbulences which could be integrated according to [16].

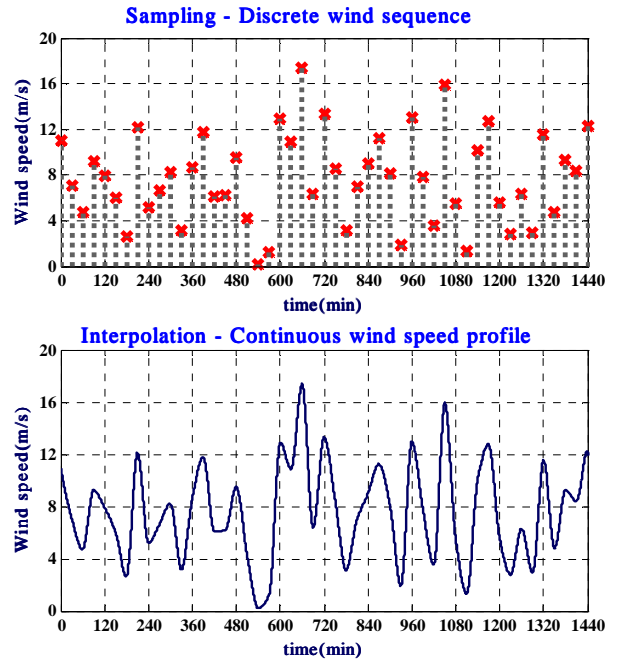


Figure 4. Generation of a wind speed profile for one day duration

### 2.3. Load demand

In this study a typical farm is considered as case study. The load profile of this farm on one day duration is illustrated in Figure 5. The highest load demands occur between 7 and 8 am and 6 and 9 pm.

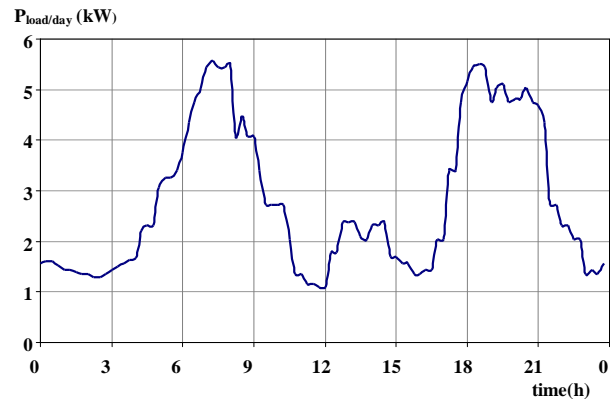


Figure 5. Typical farm load profile for one day.

## 3. PASSIVE WIND SYSTEM MODEL

### 3.1. Similitude sizing model

In [5], an integrated optimal design method based on multiobjective optimization has been developed for sizing the elements of a 1.7 kW passive wind turbine system. In our case, a simplified approach has been preferred based on the exploitation of similitude effects. The similitude sizing principle is based on the linearity of the magnetic field equations and the consideration of a constant flux density.

The new generator dimensions are related to the 'reference' bore radius  $r_{sref}$  and the machine length  $l_{rref}$  of the optimized generator. The reduced parameters  $\alpha_r$  and  $\alpha_l$  are introduced:

$$\alpha_r = \frac{r_s}{r_{sref}} \quad (3)$$

$$\alpha_l = \frac{l_r}{l_{rref}}$$

where,  $\alpha = \alpha_l = \alpha_r = \sqrt{\frac{P_{dim}}{P_{dimref}}} = 2.136$  and where the

index ref is associated with the parameters of the reference "optimal" system (i.e. the 1.7 kW wind turbine system of [5]).

Others parameters of the new machine reviewed by similitude are summarized in the table below:

**Table 1.** PMSG parameters.

Parameter	New generator
Torque $T(Nm)$	$\alpha^3 \cdot T_{ref}$
Flux (mm)	$\alpha^2 \cdot \Phi_{ref}$
Inductance $L(H)$	$\alpha \cdot L_{ref}$
Resistance $R(\Omega)$	$R_{ref}/\alpha$

Finally, using a similitude-based approach, the PMSG as well as the wind turbine features can be deduced for an 8 kW passive wind turbine system. Results obtained with this approach will be presented in section 5.

### 3.2. Wind turbine model

The mechanical wind turbine output power,  $P_{WT}(t)$  (W), generated by the wind turbine is defined as follows:

$$P_{WT} = \frac{1}{2} C_p \rho S v^3 \quad (4)$$

where  $\rho$  is the air density ( $kg \cdot m^{-3}$ ),  $S$  denotes the swept rotor area ( $m^2$ ),  $v$  represents the wind speed (m/s) and  $C_p$  is the power coefficient from manufacturer data corresponding to the turbine studied in [5] and that can be interpolated with the following expression:

$$C_p(\lambda) = -3.98 \cdot 10^{-8} \lambda^7 - 4.21 \cdot 10^{-6} \lambda^6 + 2.1 \cdot 10^{-4} \lambda^5 - 3.1 \cdot 10^{-3} \lambda^4 + 1.64 \cdot 10^{-2} \lambda^3 - 0.0176 \lambda^2 + 0.0174 \lambda - 1.93 \cdot 10^{-3} \quad (5)$$

where  $\lambda$  is the tip speed ratio which depends on the turbine rotational speed  $\Omega$  (rad/s), on the wind turbine radius  $R$  and on the wind speed  $v$ .

$$\lambda = \frac{R\Omega}{v} \quad (6)$$

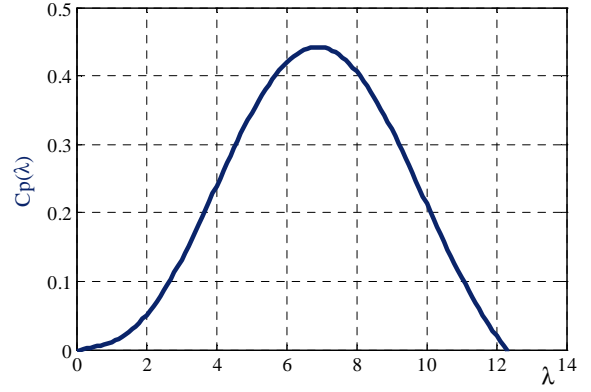


**Figure 6.** Wind turbine power coefficient.

### 3.3. Sizing model of the diode rectifier

An IXYS VUO190 [17] is considered for the diode bridge rectifier. In this study the switching losses are neglected. Thus, Power losses in the diode rectifier result from conduction losses that can be expressed as:

$$P_{cond} = 2(U_{d0} \cdot I_d + R_d \cdot I_d^2) \quad (7)$$

where,  $U_{d0}$  is the diode voltage drop and  $R_d$  represents the diode internal resistance (typically  $R_d = 2.2$  m $\Omega$  and  $U_{d0} = 0.8$  V).

### 3.4. Mixed-reduced model of the passive wind turbine system

We present in this section a simplified model of the generator associated with a diode bridge rectifier taking into account the diode overlapping during switching intervals [4, 10].

#### 3.4.1. Equivalent DC model

In this simplified causal model, the association between PMSG and the diode bridge is represented with a DC model which is energetically equivalent in terms of average values. This PMSG equivalent circuit model is shown in Figure 7.

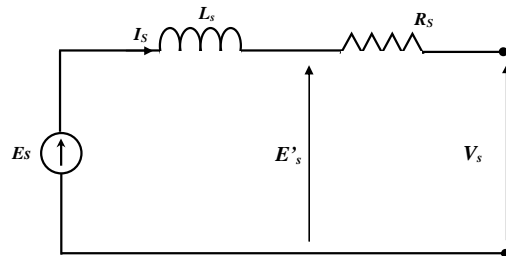


**Figure 7.** The PMSG equivalent circuit.

Figure 8 shows the synoptic of the equivalent DC model where causality is symbolized by arrows specifying which physical variables (energetic efforts or flows) are applied to each part of the system.

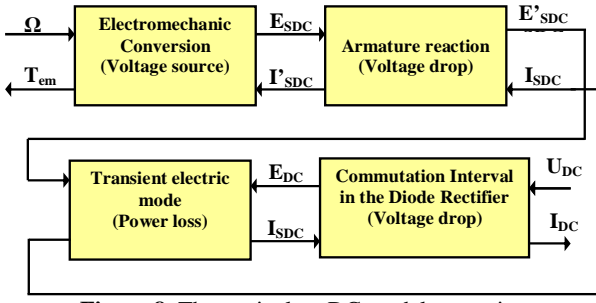


Figure 8. The equivalent DC model synoptic.

The correspondence between AC (rms) values and DC ones, in the PMSG circuit model is given in Table 2.

The electromechanical conversion is represented as follows:

$$\begin{cases} T_{em} = p \Phi_{DC} I'_{sDC} \\ E_{sDC} = p \Phi_{DC} \cdot \Omega \end{cases} \quad (8)$$

where,  $p$  is the pole pair number of the generator.

Table 2. Correspondence between PMSG circuit and equivalent DC model.

Variable	PMSG	Equivalent DC model
Voltage	$V_s$	$U_{DC} = \frac{3\sqrt{6}}{\pi} \cdot V_s$
Current	$I_s$	$I_{DC} = \frac{\pi}{\sqrt{6}} \cdot I_s$
Flux	$\Phi_s$	$\Phi_{DC} = \frac{3\sqrt{6}}{\pi} \Phi_{eff}$
Inductance	$L_s$	$L_{DC} = 3 \left( \frac{3\sqrt{6}}{\pi} \right)^2 L_s$
Resistance	$R_s$	$R_{DC} = 3 \left( \frac{3\sqrt{6}}{\pi} \right)^2 R_s$
Electromotive force	$E_s$	$E_{sDC} = \frac{3\sqrt{6}}{\pi} E_s$

The armature reaction in the generator is modelled with a voltage drop without power losses:

$$\begin{cases} E'_{sDC} = \sqrt{E_{sDC}^2 - (L_{DC} \cdot \omega \cdot I_{sDC})^2} \\ I'_{sDC} = \frac{E'_{sDC} \cdot I_{sDC}}{E_{sDC}} \end{cases} \quad (9)$$

where  $\omega$  is the electric angular pulsation of the rotor. The transient electric mode leads to a DC current in the generator defined as:

$$L_{DC} \frac{dI_{sDC}}{dt} + R_{DC} I_{sDC} = E'_{sDC} - E_{DC} \quad (10)$$

The diode overlapping during the commutation interval is represented by a power conservative voltage drop:

$$\begin{cases} U_{DC} = E_{DC} - \frac{3}{\pi} L_s \omega I_{DC} \\ I_{DC} = E_{DC} I'_{sDC} / U_{DC} \end{cases} \quad (11)$$

### 3.4.2. Mixed-reduced model

The electrical mode effect can be neglected by only considering the energetic system behaviour. Hence, we arrive to an additional model reduction. In this simplified model (called mixed-reduced model), we only simulate the mechanical modes of the system. The electrical parts are analytically derived by integration of the armature reaction with the Joule effect. The combination of equations (9) and (10) leads to:

$$I_{sDC}^2 + \frac{2U_{DC} \cdot R_{eq}}{(L_{DC} \cdot \omega)^2 + R_{eq}^2} \cdot I_{sDC} + \frac{U_{DC}^2 - E_{sDC}^2}{(L_{DC} \cdot \omega)^2 + R_{eq}^2} = 0 \quad (12)$$

where  $R_{eq} = \frac{3}{\pi} L_s \omega + R_{DC}$ .

The DC current in the diode rectifier can be obtained by solving equation (12).

### 3.4.3. PMSG losses model

The PMSG presents three kinds of losses: copper losses, iron core losses, and mechanical losses [11-13]. Copper losses are the heat losses in the windings due to their electrical resistance. The copper losses are proportional to the square of the current.

$$P_j = 3R_s I_s^2 \quad (13)$$

Iron losses are due to hysteresis and eddy-current losses produced in the stator parts (i.e. yoke and teeth). Iron losses in the yoke are computed as follows:

$$\begin{cases} P_{Hyst}^{yoke} = V_{yoke} \frac{2K_H}{\pi} \hat{B}_y^2 \omega \\ P_{Hyst}^{yoke} = V_{yoke} \frac{4\alpha_p}{\pi^2 K_p} \hat{B}_y^2 \omega^2 \end{cases} \quad (14)$$

where the filling coefficient  $K_p$  is set to 0.833,  $K_H$  and  $\alpha_p$  are empirical factors depending on the material (typically  $K_H=52$  and  $\alpha_p=0.06$  for FeSi 3%). Similarly, iron losses in the teeth can be deduced by the following relation:

$$\begin{cases} P_{Hyst}^{teeth} = V_{teeth} \frac{2K_H}{\pi} \hat{B}_{teeth}^2 \omega \\ P_{Hyst}^{teeth} = V_{teeth} \frac{12\alpha_p N_{spp}}{\pi^2 K_p} \hat{B}_{teeth}^2 \omega^2 \end{cases} \quad (15)$$

where  $N_{spp}$  denotes the number of slots per pole per phase.

Mechanical losses are expressed as follows:

$$P_{mec} = f_{wt} \Omega^2 \quad (16)$$

where  $f_{wt}$  is a friction coefficient.

#### 4. BATTERY BANK SIZING METHODOLOGY

The synoptic of the battery bank sizing process is shown in Figure 9. The issue consists in producing 11 wind cycles with a progressive duration from 1 till 200 days. These cycles are synthesized from a given wind statistic (i.e. a particular Weibull distribution) during  $N_d$  days ( $N_d=1, 2, 3, 10, 20, 30, 50, 70, 100, 150$  and  $200$  days). Then, after simulation using the mixed-reduced model, 11 extracted wind powers ( $P_{wind}$ ) are generated. The load power ( $P_{load}$ ) is daily repeated during the  $N_d$  days.

The battery power defined by equation (17) is used by the sizing algorithm explained below.

$$P_{BT} = P_{wind} - P_{load} \quad (17)$$

where,  $P_{wind} = P_{WT} - \sum Losses$ .

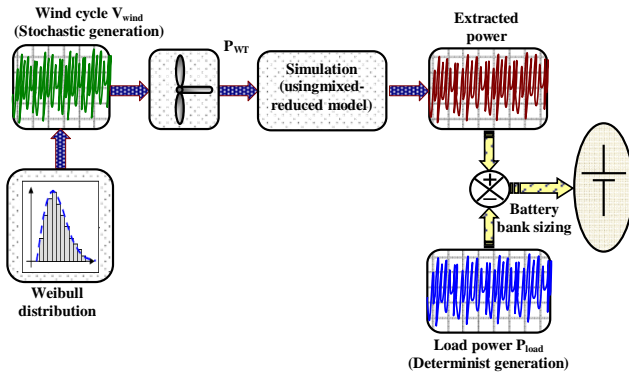


Figure 9. Battery bank sizing process.

In this study, a lead acid Yuasa NP 38-12I [18] is considered as battery element. The basic characteristics of this element are summarized in the table 3.

Table 3. Basic characteristics of a Yuasa NP 38-12I lead acid battery element.

<i>nominal capacity</i> $C_3$	<b>30,3 (Ah)</b>
<i>Nominal voltage</i> $V_0$	12 (V)
<i>nominal discharge Current</i> $I_3$	10.1(A)

The number of battery elements associated in series, to provide the desired nominal DC bus voltage is calculated as follows:

$$N_{bts} = \frac{V_{DCBUS}}{V_0} \quad (18)$$

Where  $V_{DCBUS}$  is the nominal DC bus voltage and  $V_0$  is the voltage of each element.

The number of batteries connected in series is not subject to the sizing problem. But the number of parallel battery strings  $N_{bt}$  (consisting of  $N_{bts}$  batteries connected in series), connected in parallel to yield a desired system storage capacity, and is the design variable that will be sized.

The total energy which can be stored thanks to this battery element is:

$$E_{BT}^0 = C_3 \cdot V_0 \quad (19)$$

Battery charging and discharging current limitations involve two constraints related to energy storage capacity  $E_{BT}$ , maximum charging power  $P_{BT}^C$  and maximum discharging power  $P_{BT}^D$ .

$$\begin{cases} P_{BT}^C \leq E_{BT} / \mu_C \\ P_{BT}^D \leq E_{BT} / \mu_D \end{cases} \quad (20)$$

where  $\mu_D$  is the minimum duration of battery discharging at  $P_{BT}^D$  and  $\mu_C$  is the minimum duration of battery charging at  $P_{BT}^C$ . Generally,  $\mu_D$  is set to a value between 1/5 h and 1 h, while  $\mu_C$  is set to a value between 1 h and 2 h. In the case of this study  $\mu_D$  and  $\mu_C$  are both set to 1 h.

In order to optimally size the battery bank, the algorithm of figure.10 is used. This algorithm is based on an upper saturated integration method instead of a simple integration method which generally leads to a battery bank oversizing [8, 13-15].

The battery sizing process starts from the integration of the battery power mission ( $P_{BT}$ ) by initializing the battery relative energy to *isoc* (initial state of charge). At each step of calculation, the exchanged energy  $e$  is calculated. Three cases are possible.

- ✓ **Case 1:**  $e \leq 0$  ( $e$  is provided by the battery). The exchanged energy  $e$  is taken into account whatever the battery state of charge (*soc*) value. The new state of charge is lower than the previous.
- ✓ **Case 2:**  $e > 0$  ( $e$  is provided to the battery) and  $soc + e \leq isoc$  (battery can still store  $e$ ). The exchanged energy  $e$  is taken into account to charge the battery. The new state of charge is higher than the previous.
- ✓ **Case 3:**  $e > 0$  ( $e$  is provided to the battery) and  $soc + e > isoc$  (battery is full and can not store  $e$ ). The exchanged energy  $e$  is not taken into account. The new state of charge is equal to the previous one.

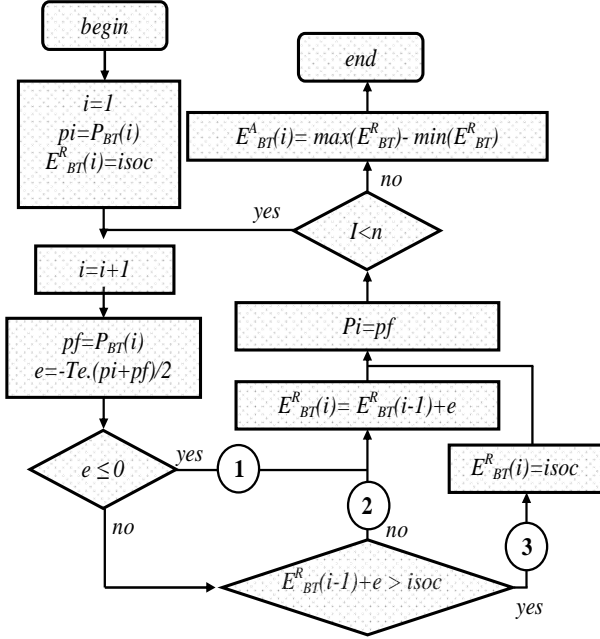


**Figure 10.** Battery active energy calculation with upper saturated algorithm.

By taking account the discharge rate  $k^{DR}$  (set to 80 % in this case); the battery energy storage capacity is given by:

$$E_{BT} = \frac{E_{BT}^A}{k^{DR}} \quad (21)$$

The number of battery elements  $N_{BT}$  is obtained by the following equation:

$$N_{BT} = \frac{E_{BT}}{E_{BT}^0} \quad (22)$$

## 5. RESULTS AND DISCUSSIONS

The similitude model is applied from the 1.7kW optimized passive wind turbine system (i.e. the 'reference system') in order obtain an 8kW passive wind turbine configuration. It should be mentioned that the similitude model is used for the generator as well as for the wind turbine.

In Tables 4 and 5, the two configuration parameters are summarized.

**Table 4.** Wind turbine parameters.

	Reference turbine	New turbine
Radius $R(m)$	1.25	2.67
Friction coefficient $f_{WT} (N.m.s/rd)$	0.025	0.52
Inertia $J_{WT}$	1.5	31.22
$C_p$ at MPPT $C_{p,opt}$	0.441	0.441
$\lambda$ at MPPT $\lambda_{opt}$	6.9	6.9

**Table 5.** PMSG parameters.

	Reference generator	New generator
Teeth width $w_t (mm)$	5.465	11.672
Yoke thickness $d_y (mm)$	14.096	30.098
Number of pole pairs $p$	3	3
Number of slots per phase per pole $N_{spp}$	3	3
Leakage inductance $L_f (mH)$	0.224	0.118
Main inductance $L_m (mH)$	0.763	0.731
Stator inductance $L_s (mH)$	1.369	1.2
Stator flux $\Phi_s (Wb)$	0.211	0.4708
Stator resistance $R_s (\Omega)$	0.128	0.0148

Figure 11 shows the extracted power of the new passive wind turbine system obtained by similitude. It can be seen that this passive configuration matches very closely the behaviour of active wind turbine systems operating at optimal wind powers by using an MPPT control device (i.e. the cubic curve on Figure 11).

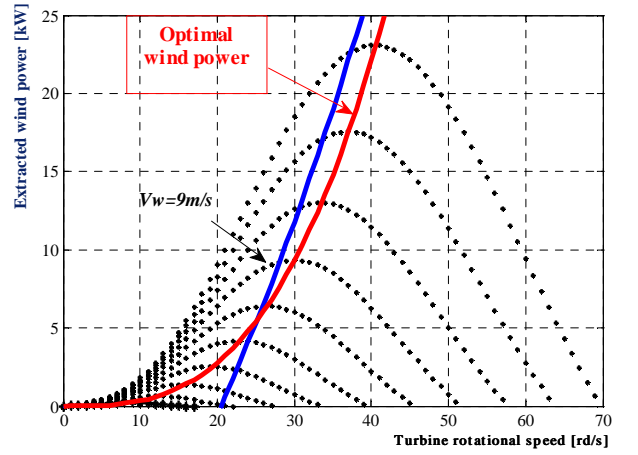


**Figure 11.** Extracted power of the new passive wind turbine system.

Several simulations of the 11 wind cycles (with an increasing number of days from 1 to 200) have been performed to taking account stochastic nature of wind. Hence, the number of batteries  $N_{bt}$  given in table 6 is the average number of batteries obtained after 10 simulations. The standard deviation  $\sigma$  of  $N_{bt}$  obtained for the 11 generated wind cycles are also given.

**Table 6.** Number of batteries and standard deviation.

Number of days	$N_{bt}$	$\sigma$
1	46	0.98
2	54	1
3	61	1.1
10	88	1.5
20	97	1.41
30	109	1.76
50	117	1.66
70	129	2.1
100	126	2.2
150	126	2
200	130	2.3

The number of batteries obtained from the 11 generated wind cycles is shown in Figure 12.

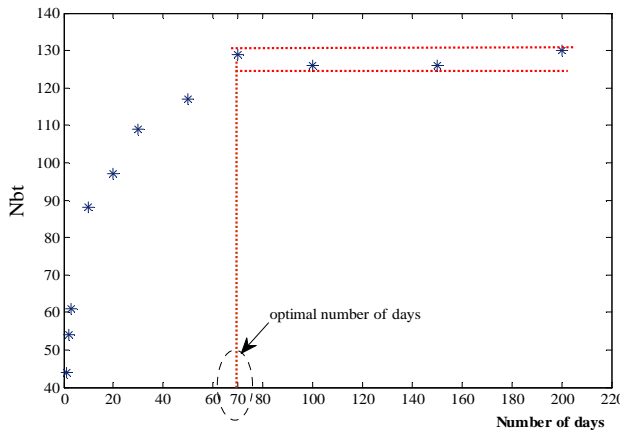


Figure 12. Plot of batteries numbers versus cycle duration.

A first analysis of these results shows that  $N_{bt}$  becomes quasi-constant and does not exceed 132 battery elements for  $N_d > 70$  days. This “optimal duration threshold” is sufficient in order to take into account wind variability (i.e. stochastic features of wind) and to obtain a suitable and robust sizing for the battery bank.

## 6. CONCLUSION

In this paper, a methodology for sizing a battery bank devoted to a stand alone wind turbine system has been developed. The passive structure of the wind turbine, minimizing the number of sensors and the electronic part, has been chosen because of its reliability and its low cost. The proposed sizing approach takes into account stochastic features of wind energy potential in a particular location with a given deterministic power demand. This approach is based on the exploitation of wind speed distribution from a Weibull law. It has been shown that a robust sizing of the battery bank can be obtained from the stochastic simulation of the extracted wind power and from the evaluation of all losses in the system using a specific algorithm. This algorithm determines, inside a given time window, the required active energy of the battery by using an upper saturated integration of the battery power.

## References

[1] Bouscayrol A, Delarue Ph, Guillaud X. “Power strategies for maximum control structure of a wind energy conversion system with a synchronous machine”. *Renewable Energy* 2005; 30(15):2273–88.  
 [2] T. Senjyu, D. Hayashi, A. Yona, N. Urasaki, T. Funabashi, “Optimal configuration of power generating systems in isolated island with renewable energy”, *Renewable Energy* 2007, Vol 32, pp. 1917-1933.  
 [3] Mirecki A, Roboam X, Richardeau F. “Architecture cost and energy efficiency of small wind turbines:

which system tradeoff?” *IEEE Transactions on Industrial Electronics*, February 2007;54(1):660–70.

[4] J. L. Bernard-Agustín, R. Dufo-Lopez, D. M. Rivas-Ascaso, “Design of isolated hybrid systems minimizing costs and pollutant emissions”, *Renewable Energy*, Vol.31, No. 14, November 2006, pp. 2227-2244.  
 [5] D.H. Tran, B. Sareni, X. Roboam, C. Espanet, “Integrated Optimal Design of a Passive Wind Turbine System: An experimental validation”, *IEEE Transactions on Sustainable Energy*, Vol. 1, n°1, pp. 48-56, 2010.  
 [6] B.S. Borowy, Z.M. Salameh, “Methodology for optimally sizing the combination of a battery bank and PV array in a Wind/PV hybrid system”, *IEEE Transactions on Energy Conversion*, Vol. 11, No. 2, June 1996.  
 [7] A.D. Bagul, Z.M. Salameh, B.S. Borowy, “Sizing of a stand-alone hybrid wind-photovoltaic system using a three-event probability density approximation”, *Solar Energy*, Vol. 56, No. 4, 1996.  
 [8] R. Belfkira, C. Nichita, P. Reghem, G. Barakat, “Modeling and optimal sizing of hybrid energy system”, *International Power Electronics and Motion Control Conference (EPE-PEMC)*, September 1-3, 2008, Poznan, Poland.  
 [9] J.K. Keller, “Simulation of Wind with ‘K’ Parameter”, *Wind Engineering*, Vol. 16, No 6, p. 307-312, 1992.  
 [10] B. Sareni, A. Abdelli, X. Roboam, D.H. Tran, “Model simplification and optimization of a passive wind turbine generator”, *Renewable Energy* 2009.  
 [11] Y.-K. Chin, J. Soulard “Modelling of iron losses in permanent magnet synchronous motors with field weakening capability for electric vehicles” *International Journal of Automotive Technology*, Vol. 4, No. 2, pp. 87–94 (2003)  
 [12] Hoang E, Multon B, Gabsi M. “Enhanced accuracy method for magnetic loss measurement in switched reluctance motor”. *ICEM’94* 1994;2:437–42.  
 [13] C.R. Akli, X. Roboam, B. Sareni, A. Jeunesse, “Energy management and sizing of a hybrid locomotive”, *12th International Conference on Power Electronics and Applications (EPE’2007)*, Aalborg, Denmark, 2007  
 [14] R. Belfkira, G. Barakat, C. Nichita, “Sizing optimization of a stand-alone hybrid power supply unit: wind/PV system with battery storage”, *International Review of Electrical Engineering (IREE)*, Vol. 3, No. 5, October 2008.  
 [15] S. Piller, M. Perrin, A. Jossen, “Methods for state-of-charge determination and their applications”, *Journal of Power Sources, Elsevier*, 2001, pp. 113-120.  
 [16] X. Roboam, A. Abdelli, B. Sareni, “Optimization of a passive small wind turbine based on mixed Weibull-turbulence statistics of wind”, *Electrimacs* 2008, Québec, Canada, 2008.  
 [17] <http://www1.futureelectronics.com/doc/IXYS>  
 [18] <http://www.houseofbatteries.com/pdf/NP38-12>